Polymer Chemistry

ROYAL SOCIETY OF CHEMISTRY

PAPER

View Article Online
View Journal | View Issue

Cite this: *Polym. Chem.*, 2021, **12**, 196

Solubility-governed architectural design of polyhydroxyurethane-*graft*-poly(ε-caprolactone) copolymers†

Charalampos Pronoitis, Minna Hakkarainen and Karin Odelius *

Polyhydroxyurethanes (PHUs) are strong candidates for replacing conventional isocyanate-based polyurethanes (PUs), yet analogous structural diversity and subsequent properties have so far not been reached for PHUs. Here, we demonstrate that by rational design of the PHU microstructure and utilization of solubility as an enabling tool, complex architectures can be realized with benign reagents and atom-economical reactions, without harsh reaction conditions and solvents. Polyhydroxyurethane-*graft*-poly(ε-caprolactone), PHU-*graft*-PCL, copolymers were synthesized through graft ring-opening polymerization of ε-caprolactone (CL) from the pendent –OH groups of a PHU. The structure of the PHU was carefully designed to allow its dissolution in CL and enable bulk polymerization conditions. Solubility tests of different PHUs in various lactones corroborated that the PHU-lactone structure pair was critical to achieve dissolution. The optimum reaction conditions were kinetically determined, the copolymers' structure was confirmed by ^{1}H, DOSY and ^{31}P NMR spectroscopy and their thermal properties were evaluated by DSC and TGA analysis. Our work demonstrated the effectiveness of utilizing solubility to achieve complex architectures, expanding the synthetic intricacy for PHUs and could expand their future applications and opportunities.

Received 30th July 2020,
Accepted 31st October 2020

DOI: 10.1039/d0py01089h

rsc.li/polymers

Introduction

Significant effort is undertaken to develop solvent-free, atom-economical synthetic procedures, utilizing benign reagents and mild conditions as alternatives for the production of conventional polymers. There is also an ongoing quest to decrease the oil dependence of the chemical industry and therefore, great interest lies in exploiting renewable resources to obtain platform chemicals that can serve as precursors to functional monomers and polymers. One such "greener" class of polymers is polyhydroxyurethanes (PHUs). PHUs have emerged as a safer alternative to conventional thermoplastic and thermoset polyurethanes (PUs) that utilize toxic isocyanates for their production.[1] The most common synthesis route to create PHUs is step-growth polymerization between diamines and cyclic dicarbonates, a highly attractive method from a sustainability point of view. It is atom-economical, it can be performed under bulk conditions and can be combined with extrusion techniques[2,3] to shorten the polymerization time needed and improve the final characteristics of the PHUs. Structural diversity in the linear and crosslinked PHUs can also be achieved by utilizing one of the numerous dicarbonate precursors in combination with one or more of the several diamines available. These building blocks can be derived from renewable resources,[4,5] enabling biobased PHUs with tailored microstructure, designed to reach the properties needed for the intended application. A plethora of cyclic carbonates can be accessed by incorporating CO_2 to oxiranes[6,7] and oxetanes[8] or benign carbonylating agents such as dimethyl carbonate to diols[9,10] thereby avoiding toxic phosgene and contributing to the fixation of CO_2 for materials' production.[11]

Much fewer examples exist, however, of PHUs combined with other classes of polymers, creating more complex structures such as block, star or graft copolymers. This could be due to the inherent challenge of synthetic control over step-growth polymerization, the low molar masses achieved and the limited solubility of PHUs caused by the hydrogen bonding (H-bonding).[12,13] Carbonate, ester and ether,[14] thioether,[15] sulfone,[16] siloxane,[17] amide[18] and tertiary amine[19] groups or longer segments of oligo-esters, -ethers and -carbonates,[20,21] have for instance been reported along the backbone of linear PHUs, yielding diverse microstructures. Hydroxyurethane moieties have also been incorporated as side-groups in fluorinated, alternating copolymers[22] and polyester-*graft*-poly(ethylene glycol) brush copolymers,[23] and recently biobased ester-

Department of Fibre and Polymer Technology, KTH Royal Institute of Technology, Teknikringen 56-58, 100 44 Stockholm, Sweden. E-mail: hoem@kth.se

†Electronic supplementary information (ESI) available. See DOI: 10.1039/d0py01089h

urethane star polymers based on glycerol and dimethyl-2,5-furan dicarboxylate were reported.[24] Hence, PHUs with diverse microstructures can be achieved and hydroxyurethane functionalities can be used to decorate various polymer backbones, but copolymers with a PHU block or more complex architectures are lacking, especially when considering synthesis conditions devoid of solvents and hazardous reagents.

To truly promote sustainable polymers, in addition to utilizing benign reactants and mild reaction conditions, it is critical to prove that they are not limited to linear or crosslinked structures, but that they can be utilized for the synthesis of functional copolymers with complex architecture even for 'hard to work with' systems. We hypothesized that the flexibility of the PHU chemistry could enable this. By designing a biobased PHU with a microstructure that would allow its dissolution in ε-caprolactone (CL), a brush-like copolymer could be created by graft ring-opening polymerization (ROP) of CL from the pendent hydroxyl groups of the PHU and the copolymer characteristics could be simply controlled by adjusting the monomer : initiator ratio. 2,2′-(Ethylenedioxy)bis(ethylamine) (EDOBA) and diglycerol carbonate (DGC) were selected as monomers for the PHU. This selection had twofold importance. First, DGC can be easily synthesized from renewable, benign and inexpensive diglycerol and dimethyl carbonate, thereby, the sustainability requirements are met. Second, it bears an ether bridge which in combination with the ethylene glycol moiety of EDOBA should favor the dissolution of the PHU in CL allowing for bulk polymerization conditions and achieving an overall more sustainable synthesis.

Experimental

Materials

All reagents were used as received without further purification, unless stated otherwise. Moisture- and air-sensitive reagents were stored and used under inert N_2 atmosphere in a MBraun glovebox. Diglycerol (DG, mixture of isomers, >80.0% with respect to the α,α′-isomer) was purchased from TCI Europe. Dimethyl carbonate (DMC, 99%) was purchased from Alfa Aesar. Calcium hydride (CaH_2, ≥90%), potassium carbonate (K_2CO_3, ≥99.0%), tin(II) 2-ethylhexanoate ($Sn(Oct)_2$, 92.5–100%), ε-caprolactone (CL, 97%), 2,2′-(ethylenedioxy)bis (ethylamine) (EDOBA, 98%), methanesulfonic acid (MSA, ≥99.0%), 1,5,7-triazabicyclo[4.4.0]-dec-5-ene (TBD, 98%), chromium(III) acetylacetonate ($Cr(acac)_3$, 97%), 2-chloro-4,4,5,5-tetramethyl-1,3,2-dioxaphospholane (Cl-TMDP, 95%), *N*-hydroxy-5-norbornene-2,3-dicarboxylic acid imide (HNOB, 97%), toluene (anhydrous, 99.8%), tetrahydrofuran (THF, ≥99.0%), ethyl acetate (EtOAc, ≥99.5%), butyl acetate (BuOAc, ≥99.5%), δ-valerolactone (δVL, technical grade), γ-valerolactone (γVL, 99%), ω-pentadecalactone (ωPDL, ≥98%), hexadecanolide (HDL, 97%), ethylene brassylate (EB, ≥95%), δ-decalactone (δDL, ≥98%), ε-decalactone (εDL, ≥99%) and α-bromo-γ-butyrolactone (αBr-γBL, 97%) were purchased from Sigma-Aldrich. Pyridine (≥99.7%), methanol (MeOH, ≥98.5%), *n*-heptane (≥99%), acetone (≥99%), chloroform-d ($CDCl_3$, 99.8% D) and dimethyl sulfoxide-d_6 (DMSO-d_6, 99.8% D) were purchased from VWR. Chloroform ($CHCl_3$, ≥99.8%) was purchased from Fisher Scientific. CL was stirred over CaH_2 for 24 h, distilled under vacuum and stored over activated 4 Å molecular sieves under inert atmosphere before use. $Sn(Oct)_2$ was stored over activated 4 Å molecular sieves under inert atmosphere before use.

Synthesis of diglycerol carbonate (DGC). DGC was synthesized as described by Tryznowski *et al.*[9] and purified as described by van Velthoven *et al.*[10] The adapted procedure is as follows: diglycerol (100 g, 0.60 mol, 1 eq.) and K_2CO_3 (0.5 g, 0.0036 mol, 0.006 eq.) were suspended in 300 mL of dimethyl carbonate (320 g, 3.6 mol, 6 eq.) in a 500 mL round-bottom flask and heated under reflux for 24 h. Unreacted DMC and the methanol byproduct were removed under vacuum at 65–70 °C, resulting in a light brown, viscous oil. The oil was mixed with 150 mL of deionized H_2O to remove any residues of DG and K_2CO_3 and an off-white crystalline solid precipitated. H_2O was removed by filtration and the solid was further suspended over 200 mL of MeOH and stirred for 40 min. MeOH was filtered out and the product was dried overnight in a vacuum oven yielding DGC as white, crystalline solid (65 g, 50% yield), Fig. S1.†

General procedure for the synthesis of PHUs. DGC (8 g, 0.0367 mol, 1 eq.) and EDOBA (5.43 g, 0.0367 mol, 1 eq.) were mixed in a 100 mL round-bottom flask at room temperature and subsequently heated in an oil bath at 100 °C, under mechanical stirring for 24 h. The reaction was thermally quenched by placing the flask in liquid N_2. The PHU was removed and stored at room temperature until further use.

Estimation of hydroxyl group content of the PHUs. The −OH content of the PHU was calculated through ^{31}P NMR spectroscopy, after phosphitylation of the −OH groups with 2-chloro-4,4,5,5-tetramethyl-1,3,2-dioxaphospholane (Cl-TMDP), as previously described.[25–27]

Effect of catalyst on the PHU. Three solutions of 25 mg of PHU in 0.7 mL of DMSO-d_6, were prepared in snap-on lid glass vials. To each of them, a stirring bar and 5 mol% respect to the PHU, of TBD, MSA and $Sn(Oct)_2$ were added, respectively. The vials were placed in an oil bath, at 120 °C for 24 h under stirring. A PHU solution without any catalyst was prepared the same way and used as reference. After, the solutions were cooled down, they were transferred to NMR tubes and analyzed with ^{13}C NMR spectroscopy.

Graft ring-opening polymerization of CL. The graft ring-opening polymerization (graft ROP) of CL was monitored using MSA and $Sn(Oct)_2$ as catalysts at different loadings, and with various CL concentrations. All glassware used were dried at 130 °C for at least 24 h prior to use. The PHU was dried under vacuum overnight and then stored in a glovebox. A reaction with 100 : 1 : 0.02 of CL : OH : $Sn(Oct)_2$ ratio is described as a representative example. Inside the glovebox, 3.25 g of CL (100 CL monomers per −OH) and 50 mg of PHU (0.285 mmol of −OH) and a stirring bar were added in a 25 mL Schlenk flask and sealed with a glass stop. The flask was taken out of

the glovebox, connected to a Schlenk line and placed in a thermostated oil bath at 110 °C under stirring. A N_2 gas flow was applied and kept during the entire reaction. A solution of Sn $(Oct)_2$ (2.3 mg, 0.0057 mmol, 0.02 eq. per −OH) in a minimum amount of anhydrous toluene was added to the flask after the PHU had completely dissolved in the CL. Time zero was set as the time when all of the catalyst had been added. At regular time intervals, samples were withdrawn with oven-dried, glass Pasteur pipettes and directly dissolved in $CDCl_3$ for further ^1H NMR analysis. Once the reaction was completed, the crude product was cooled down to room temperature and purified by two successive precipitations from $CHCl_3$, first in a 10-fold excess of cold MeOH, and then in cold heptane. The solvent was filtered out and the copolymer was dried under vacuum at room temperature and stored. For the MSA-catalyzed reactions, the same procedure was followed, only MSA was directly added in the flask with an automatic pipette, and a $CDCl_3$ with 0.1 M pyridine solution was employed to quench the catalyst. Table S1† summarizes the masses of the reactants for all the kinetic reactions.

The same procedure was followed for the synthesis and purification of the copolymers under the optimized conditions with $Sn(Oct)_2$ as catalyst, but crimp-top glass vials sealed with butyl/PTFE septum caps were employed instead of Schlenk flasks. The masses of the reactants for these reactions are summarized in Table S2.†

Characterization

Nuclear magnetic resonance (NMR). ^1H and ^{13}C NMR spectra were recorded at room temperature with a Bruker Avance 400 NMR spectrometer at 400 and 100 MHz, respectively, and the residual solvent signals of $CDCl_3$ (7.26, 77.16 ppm) and DMSO-d_6 (2.50, 39.5 ppm) were taken as internal reference. ^{31}P NMR spectra were recorded with the same instrument, taking as a reference the chemical shift of the hydrolysis byproduct between Cl-TMDP and moisture at 132.2 ppm. 256 scans were recorded and the relaxation time was set to 5 s. 2D diffusion-ordered spectroscopy (DOSY) experiments were performed on a Bruker DMX-400 spectrometer using a 5 mm inverse broadband probe head with a gradient coil. The probe temperature was measured by a calibrated Pt-100 resistance thermometer and adjusted using a Bruker Eurotherm variable temperature control unit. The diffusion NMR experiments were performed with a Pulsed-field gradient stimulated echo (PFG-STE) sequence. The data were recorded with a diffusion delay (Δ) varying between 30 and 180 ms and a diffusion-encoding gradient pulse duration (δ) of 5 ms using 16 scans. The gradient stabilization delay after the gradient pulse was 1 ms. Typically, 16 values of diffusion-encoding gradient were applied linearly between 2 and 57 G cm^{-1}. All NMR data were processed with MestReNova v. 9.0 software.

Size exclusion chromatography (SEC). The number and mass-average molar mass (M_n and M_w) and dispersity ($Đ$) of the polymers were evaluated by size exclusion chromatography (SEC). The pure PHUs were analyzed with a TOSOH EcoSEC HLC-8320GPC system, equipped with an EcoSEC RI detector and three columns from PSS GmbH (PSS PFG 5 μm; microguard, 100 Å and 300 Å). The mobile phase was DMF with 0.01 M LiBr at 50 °C, at a flow rate of 0.2 mL min^{-1}. A conventional calibration method was created using narrow poly (methyl methacrylate) standards ranging from 700 to 2 000 000 g mol^{-1}. PSS WinGPC Unity v. 7.2 software was used to process the data. For the PHU-*graft*-PCL copolymers, a Malvern GPCMAX instrument was employed equipped with a PLgel 5 μm guard column (7.5 × 50 mm), two PLgel 5 μm MIXED-D (300 × 7.5 mm) columns and a Viscotek VE3580 RI detector. The mobile phase was $CHCl_3$ at 35 °C, at a flow rate of 0.5 mL min^{-1} and toluene was used as internal standard for flow rate fluctuation corrections. The system was calibrated with narrow poly(styrene) standards with molar mass range from 1200 to 940 000 g mol^{-1}. The data were processed by OmniSEC v. 5.1 software.

Differential scanning calorimetry (DSC). The thermal properties of the PHU and PHU-*graft*-PCL copolymers were evaluated with differential scanning calorimetry (DSC) on a Mettler Toledo DSC 1 instrument, under a 50 mL min^{-1} N_2 flow and a 10 K min^{-1} temperature ramp. Samples (5–8 mg) were weighed in 100 μL aluminium crucibles and subjected to two heating and one cooling scan. The first heating scan was set from 25 °C to 120 °C for the copolymers, and to 150 °C for the pure PHU, followed by an isothermal stay for 2 min before cooling to −80 and −30 °C, respectively, and keeping the temperature steady for another 2 min. Finally, the temperature was raised again to 120 or 150 °C. The glass transition (T_g) and melting (T_m) temperatures were obtained from the second heating scan as the midpoint of the glass transition and the maximum of the melting peak, respectively. All values are reported as average of triplicate measurements. The degree of crystallinity (X_c) was calculated through (1):

$$X_c = \frac{\Delta H_m}{\Delta H_m^0} \times 100\% \quad (1)$$

where ΔH_m is the melting enthalpy of the sample, and ΔH_m^0 is the melting enthalpy for 100% crystalline PCL (139.5 J g^{-1}).[28] The data were processed with Mettler Toledo STARe v. 15.00 software.

Thermal gravimetric analysis (TGA). A DSC-TGA 1 instrument (Mettler-Toledo) was employed to assess and compare the thermal stability of the PHU and the PHU-*graft*-PCL copolymers. 5–10 mg of the samples were weighed in 70 μL alumina pans and heated from 50 to 600 °C, under a 50 mL min^{-1} N_2 flow and a 10 K min^{-1} temperature ramp. The onset decomposition temperature ($T_{d,\ 5\%}$) was taken at 5% mass loss. The data were processed with Mettler Toledo STARe v. 15.00 software.

Results and discussion

Graft copolymers, PHU-*graft*-PCL, were successfully designed and synthesized implementing a "grafting from" approach

through bulk, graft ROP of ε-caprolactone (CL) from the pendent –OH groups of a polyhydroxyurethane (PHU). As PHUs are very versatile with respect to the chemical structure of their building blocks and thereby their microstructure, the predefined choice of 2,2′-(ethylenedioxy)bis(ethylamine) (EDOBA) and diglycerol carbonate (DGC) allowed tailoring a PHU that was soluble in the monomer CL, thereby enabling bulk polymerization, Scheme 1.

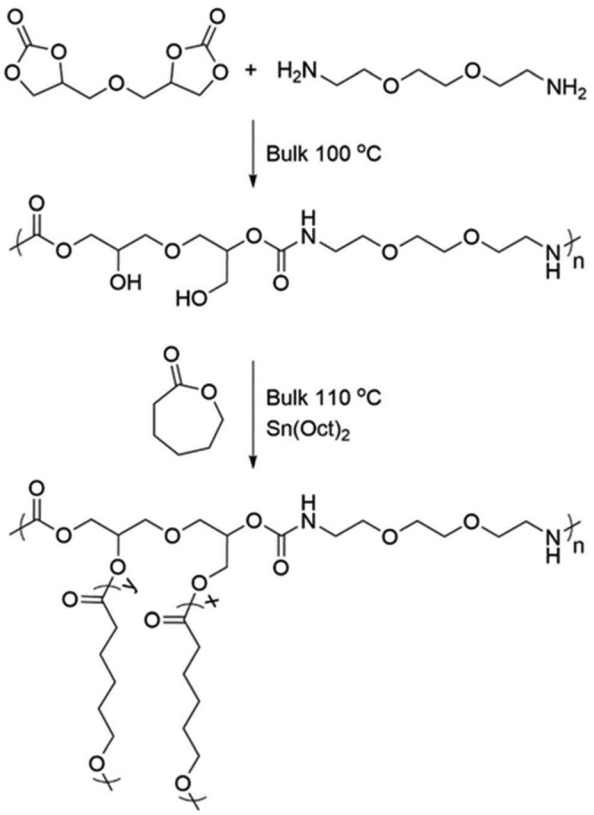

Scheme 1 Synthesis of the EDOBA PHU and the PHU-*graft*-PCL copolymers.

Polyhydroxyurethane (PHU) synthesis and characterization

As a first step towards the PHU-*graft*-PCL copolymers, the PHU main chain was synthesized under rather mild reaction conditions, 100 °C, in bulk, without the addition of catalyst and with stoichiometric balance between DGC and EDOBA.

Thanks to the comparably mild reaction conditions, the undesired side-reactions, mainly urea formation, common during PHUs' synthesis,[7,12,13,29,30] were circumvented and only <2% urea was formed. The chemical structure of the PHU was confirmed by ^{1}H NMR spectroscopy and all signals are attributed to the desired PHU structure. An overlap of the –CHCH_2O– and –CHCH_2OH protons of DGC with the –OCH_2CH_2O– protons of the diamine was observed, giving a sharp peak at 3.49 ppm, Fig. 1. The ratio of primary to secondary hydroxyl groups, pOH : sOH was 27 : 73, in agreement with other PHUs reported in the literature.[10,31–35] The pOH : sOH ratio is especially important in this system for the second step of the graft ROP, where pOH is considered a more active initiator than sOH.[36,37] The urea byproducts (<2%) were identified by the characteristic –N*H*CON*H*– protons at 5.98 ppm,[38] Fig. 1. The synthesized PHU was water-soluble and completely amorphous with glass transition temperature (T_g) of 9.6 ± 1.6 °C. The number-average molar mass (M_n) and dispersity ($Đ$) were 5300 g mol^{-1} and 1.9, respectively. The total –OH concentration of the PHU was 5.7 mmol g^{-1}, calculated through ^{31}P NMR spectroscopy after phosphitylation of the hydroxyl groups with Cl-TMDP,[26,27] Fig. S2.† Additionally, the pOH : sOH ratio was 32 : 68 which is in good agreement with the ratio determined from ^{1}H NMR spectroscopy.

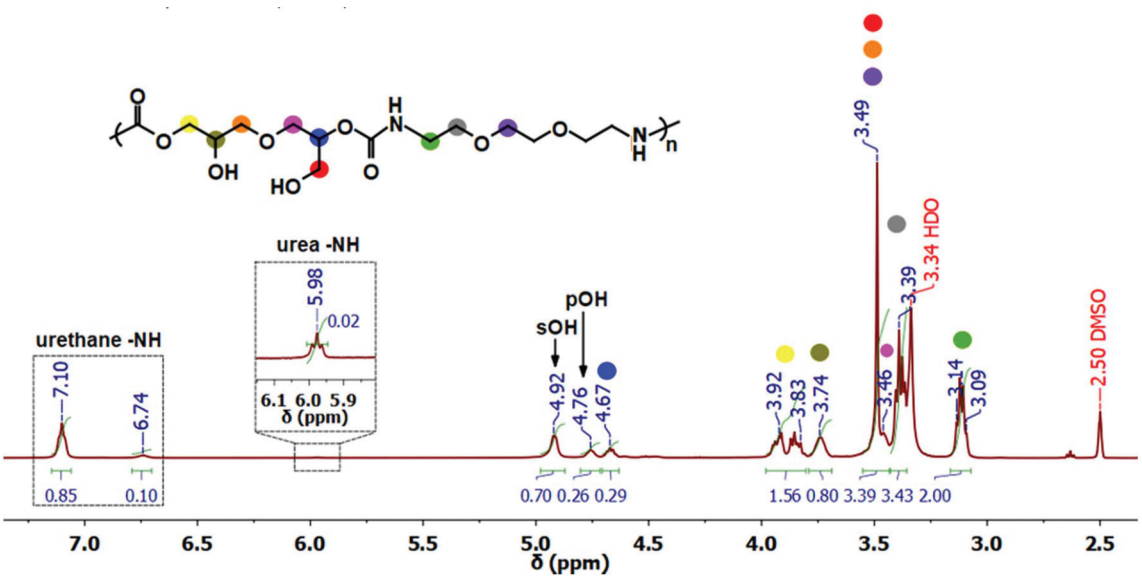

Fig. 1 ^{1}H NMR spectrum (400 MHz, DMSO-d_6) of the EDOBA PHU.

Designing the graft ROP of CL from the PHU

To achieve a complex brush-like architecture in a sustainable manner, the inherent and extensive H-bonding in the PHU[13] needs to be overcome. Protic or polar aprotic solvents such as MeOH, DMF and DMSO disrupt the intermolecular H-bonding between the pendent hydroxyl groups, acting as Lewis acid or base,[39] respectively, allowing the dissolution even in less polar $CHCl_3$.[13,32] The carbonyl oxygen of CL could potentially act as a H-bonding acceptor, similar to a solvent with an available lone electron pair, facilitating the disruption of the intermolecular H-bonding of the PHU. Combined with elevated temperature, which further contributes to the disruption of the H-bonding, the PHU could ultimately be dissolved in CL. This would create appropriate conditions for a robust, solvent-free, ring-opening polymerization of CL. To test this hypothesis, the EDOBA PHU (10 wt%) was mixed with CL at 90 °C and a slow dissolution was observed, further improved by increasing the temperature to 100 and 110 °C. At 110 °C, the PHU dissolved completely in CL and a clear solution was retained for several hours at that temperature. Upon cooling, the PHU gradually precipitated out. At low PHU concentrations (1 wt%), no precipitation was observed during cooling even after one week at room temperature.

To prove the contribution of CL's structure to the dissolution of the PHU, the solubility of the PHU was investigated in the linear equivalent of CL, butyl acetate (BuOAc) at 110 °C. Visually, the PHU was insoluble in BuOAc. The differences in solubility parameters ($\Delta\delta$) between EDOBA PHU, CL and BuOAc were calculated by Hoy's method of group contribution, providing a theoretical explanation for the observed behavior, Table S3.†[40–43] The $\Delta\delta_{PHU-CL}$ is 7.3 $(MJ\ m^{-3})^{1/2}$ and the $\Delta\delta_{PHU-BuOAc}$ is 11.4 $(MJ\ m^{-3})^{1/2}$. Both values are higher than the 5 $(MJ\ m^{-3})^{1/2}$ threshold below which the polymer is soluble in a solvent,[43] but clearly, dissolution in CL is favored over BuOAc. The high temperature applied (110 °C) has probably a beneficial effect towards dissolution, but the discrepancy could be further related to the structure of the solvent. The linear structure of BuOAc makes the alkyl groups more accessible and the polar interactions between the PHU and the CL's carbonyl oxygen may be hindered. In contrast, the ring structure of CL could be responsible for the adoption of a more favorable conformation that suppresses the freedom of movement of the alkyl groups and allows for more interactions between the carbonyl oxygen of CL and the H-bonding donor sites of the PHU, Fig. S3.† Additionally, although the ester groups of both CL and BuOAc are described as of moderate H-bonding capability,[44] lactones are more basic than linear esters due to conformational differences.[45] This increased basicity could result in slightly stronger H-bonding of CL compared with BuOAc and therefore, the ability to dissolve the PHU would be influenced as well. Ethyl acetate (EtOAc) was also evaluated near its boiling point (77 °C) due to its structural similarity with CL[46] and with the possibility that the shorter ethyl group could facilitate dissolution. The PHU was, however, again insoluble, suggesting that either the lower temperature prevents dissolution or that the same effect as for BuOAc occurs.

To further evaluate whether the microstructure of the PHU or the elevated temperature was the sole reason for dissolution in CL, we compared the solubility of a PHU with an aromatic backbone in CL. The aromatic PHU was synthesized under the same polymerization conditions as DGC and EDOBA but *m*-xylylenediamine (*m*XDA) was employed instead of EDOBA (M_n = 3500 g mol^{-1}, $Đ$ = 2.5, T_g = 37 ± 1.1 °C). Even after prolonged heating at 130 °C in CL, a considerable part of the *m*XDA PHU was not dissolved, as visually observed, confirming that high temperature is substantially contributing to the dissolution of the PHU but the chemical structure is equally important. The polar ethylene glycol moiety of EDOBA probably favored the interactions between the EDOBA PHU and CL in contrast to the hydrocarbon structure of *m*XDA. *m*XDA PHU was also not dissolved in boiling toluene, confirming that the structural similarity between the PHU and the solvent is contributing to, yet not exclusively governing, the dissolution of the PHU and that the H-bonding has a central role in it.

To gain further insight into the dissolution of the PHU, a series of lactones with varying size and functionality was evaluated for their ability to dissolve the EDOBA PHU at 110 °C, Fig. 2. Lactones with long aliphatic segments, either in the main ring (ωPDL, HDL, EB) or as side chains (δDL, εDL), were unable to dissolve the EDOBA PHU. This is most probably due to unfavorable interactions between the polar groups of the PHU and the apolar hydrocarbon moieties of the lactones, similarly to the BuOAc effect. The insolubility in α-bromo-γ-butyrolactone (αBr-γBL) should be associated with the Br-

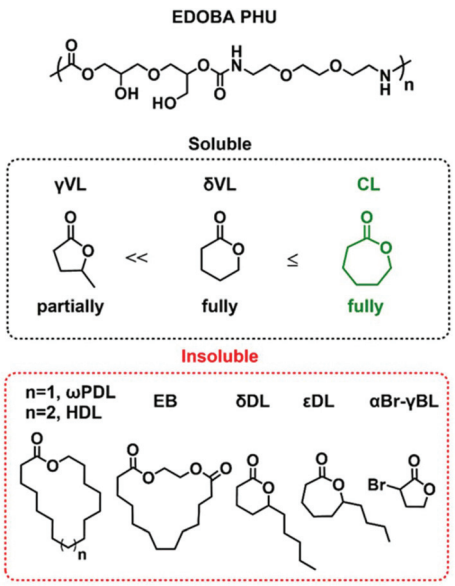

Fig. 2 Solubility of EDOBA PHU in various lactones at 110 °C. γ-valerolactone (γVL), δ-valerolactone (δVL), ε-caprolactone (CL), ω-pentadecalactone (ωPDL), hexadecanolide (HDL), ethylene brassylate (EB), δ-decalactone (δDL), ε-decalactone (εDL), α-bromo-γ-butyrolactone (αBr-γBL).

group which can act as an additional H-bonding acceptor site, but it also makes the molecule more hydrophobic. As a 6-membered ring, δ-valerolactone (δVL) could, similarly to CL, also adopt a favoring conformation that resulted in complete dissolution of the PHU after heating. However, the solution seemed less stable compared to CL and faster precipitation of the PHU occurred upon cooling, as determined by an increased haziness of the solution. The effect of the smaller ring size on dissolution was evaluated through γ-valerolactone (γVL). Low solubility was observed, with the *exo*-methyl substituent contributing to this behavior. An identical solubility test was also performed for *m*XDA PHU, which presented similar or inferior dissolution for all lactones, again highlighting the pivotal role of the PHU's microstructure.

Catalyst selection for the graft ROP of CL

To screen catalysts that enable a fast and efficient polymerization of CL, but hinder simultaneous PHU scrambling and thereby the formation of *e.g.* urea byproducts, initial trials were performed by adding catalysts to the PHU and keeping the system at 120 °C. A plethora of catalysts have been reported to efficiently catalyze the ROP of CL, ranging from metal based catalysts, such as tin- and zinc alkoxides, and pure organocatalysts, both acidic and basic such as sulfonic acids and guanidines.[47,48] To screen broadly, one of the most efficient and well-studied catalysts, tin(II) 2-ethylhexanoate ($Sn(Oct)_2$)[49] was selected along with two organocatalysts, methanesulfonic acid (MSA)[50] and 1,5,7-triazabicylco[4.4.0]-dec-5-ene (TBD).[51] The scrambling effect was evaluated by ^{13}C NMR spectroscopy monitoring changes in the carbonyl region, as it is the clearest and most direct way to determine if scrambling reactions occur. The results were compared to an uncatalyzed PHU sample heated to the same temperature, Fig. 3.

Three chemical shifts are observed for the PHU, the urethane's carbonyl carbon at 156.3 and 156.0 ppm and a small signal at 157.9 ppm corresponding to the carbonyl carbon of the urea byproduct. The –NH*C*OO– signals of the sample with no catalyst, $Sn(Oct)_2$ and MSA were completely intact after heating. In the MSA sample a new signal at 163.05 ppm appeared, most likely representing a second type of urea byproduct. This was surprising as the strong acid MSA should protonate the –OH and $–NH_2$ groups thereby, it should not allow side reactions to occur. It is possible that due to the slight basicity of DMSO, a reaction between DMSO and MSA takes place producing the corresponding salt[46] and affecting the chemical shifts of the urea byproducts that were already present. The spectrum of the TBD sample was vastly changed. The urethane signals disappeared while the 157.9 ppm signal was enhanced and a new peak at 167.6 ppm appeared. This was explained by the ability of TBD to catalyze side reactions involving the deprotonation of amine species concurrently with activation of the urethane's carbonyl and subsequent attack on the urethane bonds producing urea linkages.[38] Therefore, $Sn(Oct)_2$ and MSA were chosen as catalysts for the ROP of CL.

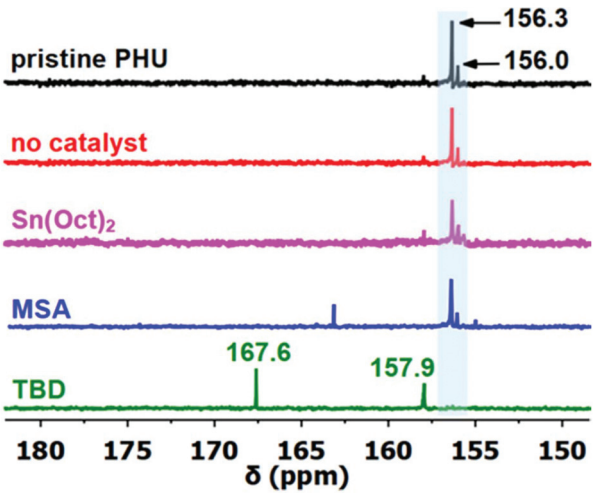

Fig. 3 Carbonyl region of ^{13}C NMR spectra (100 MHz, DMSO-d_6) of the EDOBA PHU tested with different catalysts at 120 °C.

Monitoring of the graft ROP of CL from the PHU

The kinetics of the graft ROP of CL from the PHU main chain were monitored to evaluate the efficacy of the catalysts and establish the optimum polymerization conditions for the system, varying the catalyst loading and CL loading. Initially, the CL : OH ratio was fixed at 100 : 1 and the catalyst loading was varied for both MSA and $Sn(Oct)_2$. The loadings of the catalysts were chosen based on conventional loadings of each catalyst[49,50] and to reflect the effect of higher catalyst content on the reaction rate. The MSA catalyzed polymerization of CL has been shown to occur significantly faster when the MSA : OH ratio is increased from 1 : 1 to 3 : 1, at room temperature.[50] Here, the polymerization was carried out at 110 °C and a 1 : 0.05 OH : MSA ratio was included to evaluate the influence of high temperature at a low MSA loading. Four different OH : $Sn(Oct)_2$ ratios were evaluated, 1 : 0.01, 1 : 0.02, 1 : 0.05 and 1 : 1 probing the effect of both low and high catalyst loading. A reaction temperature of 110 °C was considered ideal for the reaction to ensure full dissolution of the PHU in CL and high activity of the catalyst. The reactions were monitored by ^1H NMR spectroscopy and SEC until high conversions were reached. The samples are named after the CL and catalyst eq. per –OH group, for instance $CL_{100}MSA_1$ denotes that the reaction was catalyzed by MSA and the CL : OH and OH : MSA molar ratio was 100 : 1 and 1 : 1, respectively. The reaction conditions and characteristics of the samples are summarized in Table 1 and the conversion, M_n and $Đ$ *vs.* time profiles are presented in Fig. 4.

The reactions presented similar features; as expected increasing the catalyst loading resulted in a faster CL conversion, while in the absence of any catalyst (CL_{100}), thermal polymerization of CL took place to a small extent and after a long reaction time (4.7% conversion after 8 h), Fig. S4.† Transesterification reactions took place in the PCL blocks as indicated by the increase in $Đ$, and CL homopolymer was formed as seen from the bimodal SEC traces. Naturally,

Table 1 Reaction conditions for the kinetic study with different catalysts and catalyst loadings and characteristics of the resulting PHU-*graft*-PCL copolymers[a]

Sample name	Catalyst	CL : OH : Cat.	CL conversion [c] (%)	M_n [d] (g mol^{-1})	$Đ$[d]
CL_{100}	—	100 : 1 : —	4.7	—	—
$CL_{100}MSA_{0.05}$	MSA	100 : 1 : 0.05	9 (96)[b]	5300[e]	6.0[e]
$CL_{100}MSA_1$	MSA	100 : 1 : 1	98	36 200	2.2
$CL_{100}MSA_3$	MSA	100 : 1 : 3	98	32 500	1.8
$CL_{100}Sn_{0.01}$	$Sn(Oct)_2$	100 : 1 : 0.01	39 (98)[b]	39 500	1.7
$CL_{100}Sn_{0.02}$	$Sn(Oct)_2$	100 : 1 : 0.02	99	61 600	6.5
$CL_{100}Sn_{0.05}$	$Sn(Oct)_2$	100 : 1 : 0.05	96	62 800	7.5
$CL_{100}Sn_1$	$Sn(Oct)_2$	100 : 1 : 1	97	57 700	3.7
$CL_{10}Sn_{0.02}$	$Sn(Oct)_2$	10 : 1 : 0.02	96	Gelled (4300)[f]	Gelled (8.9)[f]
$CL_{25}Sn_{0.02}$	$Sn(Oct)_2$	25 : 1 : 0.02	96	Gelled (8200)[f]	Gelled (33.2)[f]
$CL_{50}Sn_{0.02}$	$Sn(Oct)_2$	50 : 1 : 0.02	98	71 600	8.9

[a] Total reaction time was 24 h. [b] Conversion after 72 h. [c] Calculated through $I_{4.06}/(I_{4.06} + I_{4.24–4.22})$, where $I_{4.06}$ and $I_{4.24–4.22}$ are the integrals of the –COOCH_2– signals of PCL and CL, at 4.06 and 4.24–4.22 ppm respectively, in the ^{1}H NMR spectra. [d] Values of purified samples, calculated by SEC in $CHCl_3$ against narrow PS standards. M_n values are rounded to the closest multiple of hundred. [e] The value corresponds to the crude product. [f] Sample gelled, the values in the brackets correspond to the crude fraction obtained after swelling and extraction in $CHCl_3$.

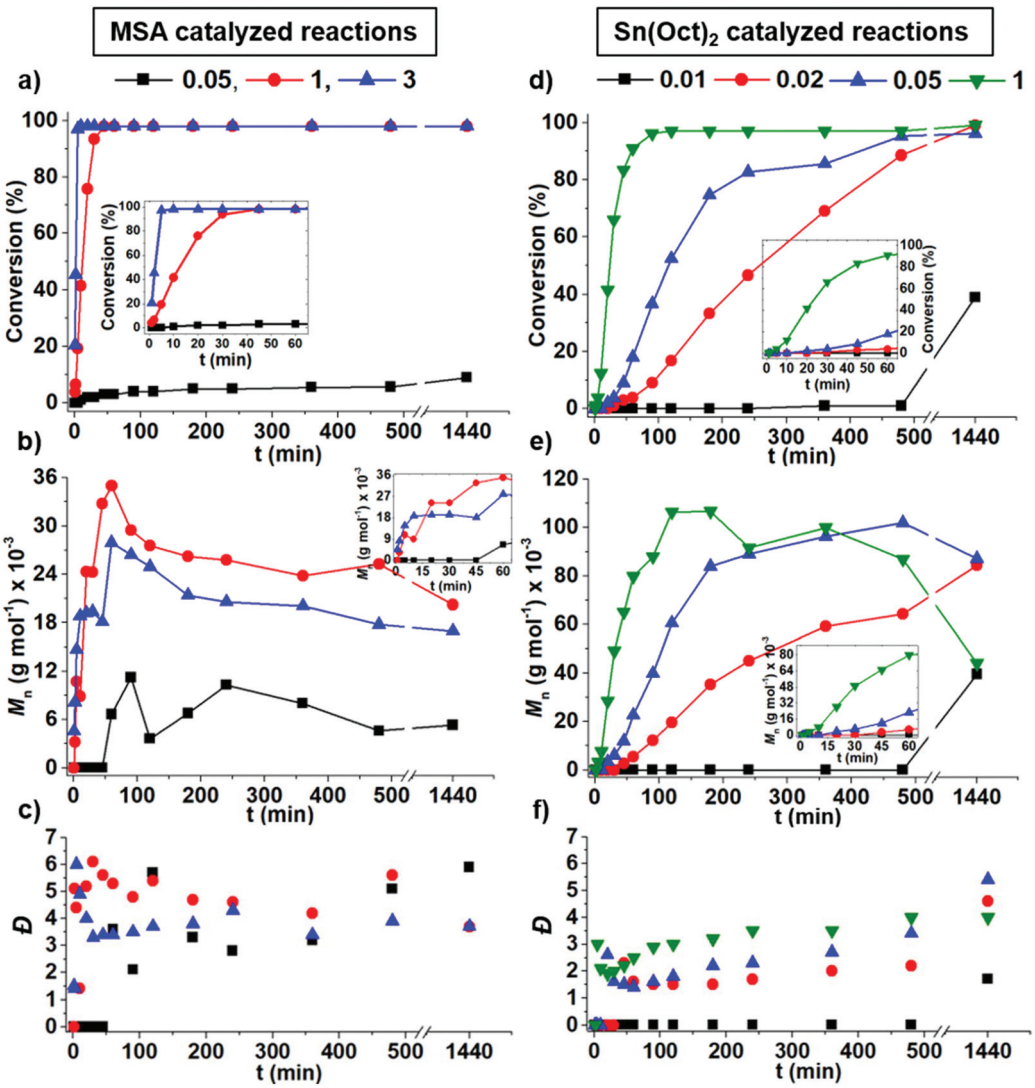

Fig. 4 Graft ROP of CL from the EDOBA PHU with varying catalyst and catalyst loading. Conversion, M_n and $Đ$ *vs.* time plots of the MSA (a, b and c) and $Sn(Oct)_2$ (d, e and f) catalyzed reactions. The CL : OH ratio was 100 : 1 and each line corresponds to the eq. of catalyst per –OH group. For clarity, the 5–60 min points of conversion and M_n *vs.* time are shown in the inset graphs.

Đ values less than ~2 are not possible as the PHU backbone already had *Đ* = 1.9. Both catalysts, at all loadings, reached high conversion at the end of the reaction, Table 1, but overall, CL's conversion was faster for the MSA than the $Sn(Oct)_2$ catalyzed reactions as seen from the conversion *vs.* time profiles in Fig. 4. $CL_{100}MSA_1$ and $CL_{100}MSA_3$ reached 98% conversion within 45 and 5 min, respectively, whereas the $CL_{100}Sn_{0.02}$, $CL_{100}Sn_{0.05}$ and $CL_{100}Sn_1$ samples achieved conversion >95% within 24, 8 and 2 h, respectively. The reason is most likely the different activation mechanisms for the two catalysts. MSA catalyzes an activated monomer mechanism by protonating the CL's carbonyl and activating the hydroxyl group by H-bonding. The reaction proceeds in two steps (nucleophilic attack and ring-opening) through a tetrahedral intermediate.[52] Instead, $Sn(Oct)_2$ follows a coordination–insertion mechanism.[49] This includes three distinct steps before the active tin alkoxide species, responsible for propagation, are generated and therefore, slower kinetics are observed. At low catalyst loading ($CL_{100}MSA_{0.05}$ and $CL_{100}Sn_{0.01}$), MSA seemed initially faster but after 24 h merely 9% conversion was reached, Table 1. In contrast, for $Sn(Oct)_2$ ($CL_{100}Sn_{0.01}$) a conversion of 39% was reached. The induction period observed is likely due to more protonation instead of activation of the –OH in the case of MSA,[50] and due to the equilibrium between the dormant chain end species and the active tin alkoxide species in the case of $Sn(Oct)_2$.[49]

The formation of the active species is favored at higher $Sn(Oct)_2$ loadings leading to faster initiation, as confirmed by $CL_{100}Sn_{0.02}$ and $CL_{100}Sn_{0.05}$. Their induction period was approximately 60 and 30 min, while the induction period of $CL_{100}Sn_1$ was ≤5 min due to the high catalyst amount, Fig. 4.

In both systems, after full conversion was reached, M_n decreased concomitantly with an increase of *Đ*. This indicated the existence of side reactions, most likely inter- and/or intramolecular transesterification, Fig. 4b, c, e and f. Transesterification is a prominent reaction in the ROP of lactones and it is largely dependent on the nature of the catalyst, reaction temperature and time. Sn-based catalysts, and specifically $Sn(Oct)_2$, are well known to induce such side reactions,[53] in linear[49,54–56] and more complex architectures such as star[57] or graft (co)polymers.[58,59] Similarly, transesterification has been observed in some sulfonic acid-catalyzed polymerizations of CL and other lactones towards linear and star-based homo- or copolymers.[60–64] Due to the abundance of hydroxyl groups and at high catalyst loadings ($CL_{100}MSA_3$, $CL_{100}Sn_1$), transesterification may take place already from the early stages of the reaction, but at a lower rate compared to the polymerization rate. In other words, the competition between transesterification and polymerization is negligible when copious CL monomer is available, but it becomes significant once high monomer conversion has been reached. This is why the low catalyst loading reactions, $CL_{100}MSA_{0.05}$ and $CL_{100}Sn_{0.01}$, did not present analogous behavior. Although prolonged reaction times open up for side reactions to occur, the conversion of those samples was low until 24 h due to the slow polymerization rate.

The achieved M_n was independent of the catalyst loading, Table 1, although the products of the MSA catalyzed reactions exhibited lower M_n values compared to the $Sn(Oct)_2$ catalyzed reactions. This was explained by the bimodal molar mass distribution observed in the SEC chromatograms, which was more pronounced for the MSA than the $Sn(Oct)_2$ catalyzed reactions and notably, it was the lowest for the $CL_{100}Sn_{0.02}$, Fig. S5 and S6.† The bimodality indicated the existence of a second species, apart from the PHU-*graft*-PCL copolymer, which could be a CL homopolymer initiated by adventitious H_2O or by 6-hydroxyhexanoic acid resulting from hydrolysis of

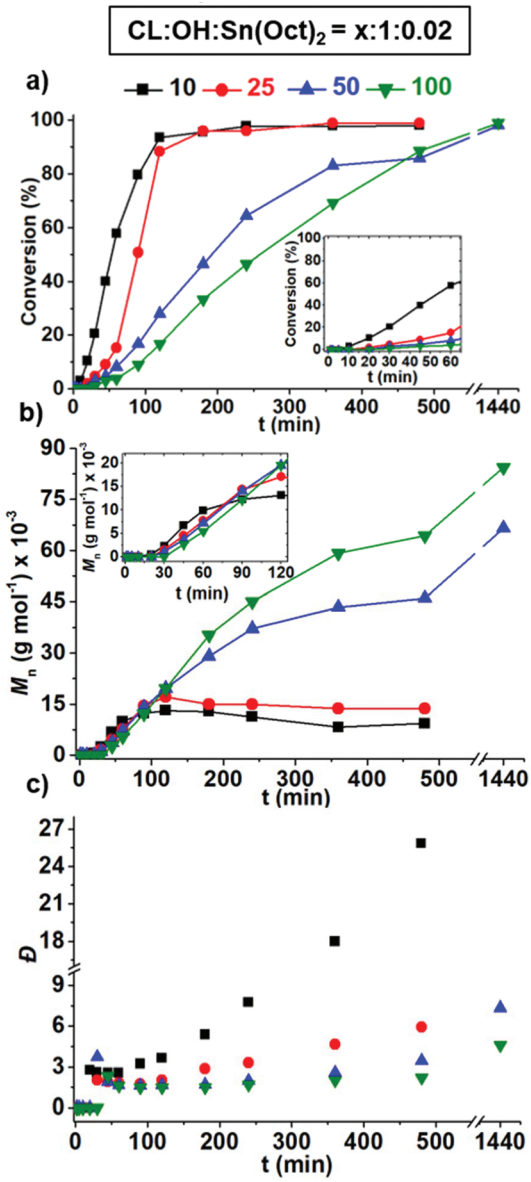

Fig. 5 Graft ROP of CL from the EDOBA PHU with varying CL loading. (a) Conversion, (b) M_n, (c) *Đ* *vs.* time plots. *x* marks the eq. of CL per –OH group. For clarity, the 5–60 min points of conversion *vs.* time and the 5–120 min points of M_n *vs.* time are shown in the inset graphs. $CL_{10}Sn_{0.02}$ and $CL25Sn_{0.02}$ samples gelled after 24 h.

CL monomer catalyzed by MSA. In either case, PCL with an α-carboxylic acid group (HOOC-PCL-OH) would be produced. The origin of the two species was determined by fractionating the 30 min sample of $CL_{100}MSA_1$ by SEC and analyzing the fractions by ^{1}H NMR spectroscopy, Fig. S7.† The spectrum of the first peak, *i.e.* the species with highest molar mass, presented a signal at 12.4 ppm, which is attributed to an acidic proton and thus, it corroborates our hypothesis. In the spectrum recorded for the second peak, the –C*H*– protons adjacent to the esterification sites are observed along with some PHU backbone signals, confirming that this species is the PHU-*graft*-PCL copolymer. The –C*H*– signals can be weakly seen in the first spectrum too, probably due to partial mixing of the two fractions during separation, Fig. S7.†

To evaluate the reactivity of the hydroxyl groups, ^{31}P NMR spectra of the purified products were recorded after –OH phosphitylation, Fig. S8.† A linear PCL synthesized in bulk with $Sn(Oct)_2$ as catalyst ($M_{n,NMR}$ = 12 200 g mol^{-1}) was taken as a reference. In the spectra of the copolymers, the PHU's –OH signals at 147.5 and 146.1 ppm have disappeared and only the terminal –OH from the PCL blocks are detected at 146.9 ppm indicating the successful graft ROP of CL from all the –OH groups. This proves that the system was not limited either by its inherent features such as steric hindrance and high viscosity of the bulk or surprisingly, by the reactivity difference between the secondary and primary hydroxyl groups. The signal at 134.7 ppm was attributed to the acid group of the CL homopolymer. The possibility of this signal belonging to

Table 2 Reaction conditions and characteristics of the final PHU-*graft*-PCL_x copolymers synthesized under the optimized conditions

x	CL : OH : $Sn(Oct)_2$	t^a (h)	CL conversion ^{b} (%)	M_n ^{c} (g mol^{-1})	$Đ^c$
10	10 : 1 : 0.02	3	96	23 200 ± 500	2.23 ± 0.01
25	25 : 1 : 0.02	3	96	42 700 ± 900	4.53 ± 0.25
50	50 : 1 : 0.02	3.5	87	75 700 ± 1100	3.50 ± 0.08
100	100 : 1 : 0.02	6	72	111 600 ± 1800	2.73 ± 0.05

^{a} Total reaction time. ^{b} Calculated through $I_{4.06}/(I_{4.06} + I_{4.24–4.22})$, where $I_{4.06}$ and $I_{4.24–4.22}$ are the integrals of the –COOCH_2– signals of PCL and CL at 4.06 and 4.24–4.22 ppm, respectively, in the ^{1}H NMR spectra. ^{c} Calculated by SEC in $CHCl_3$ against narrow PS standards, average of triplicate measurements. M_n values are rounded to the closest multiple of hundred.

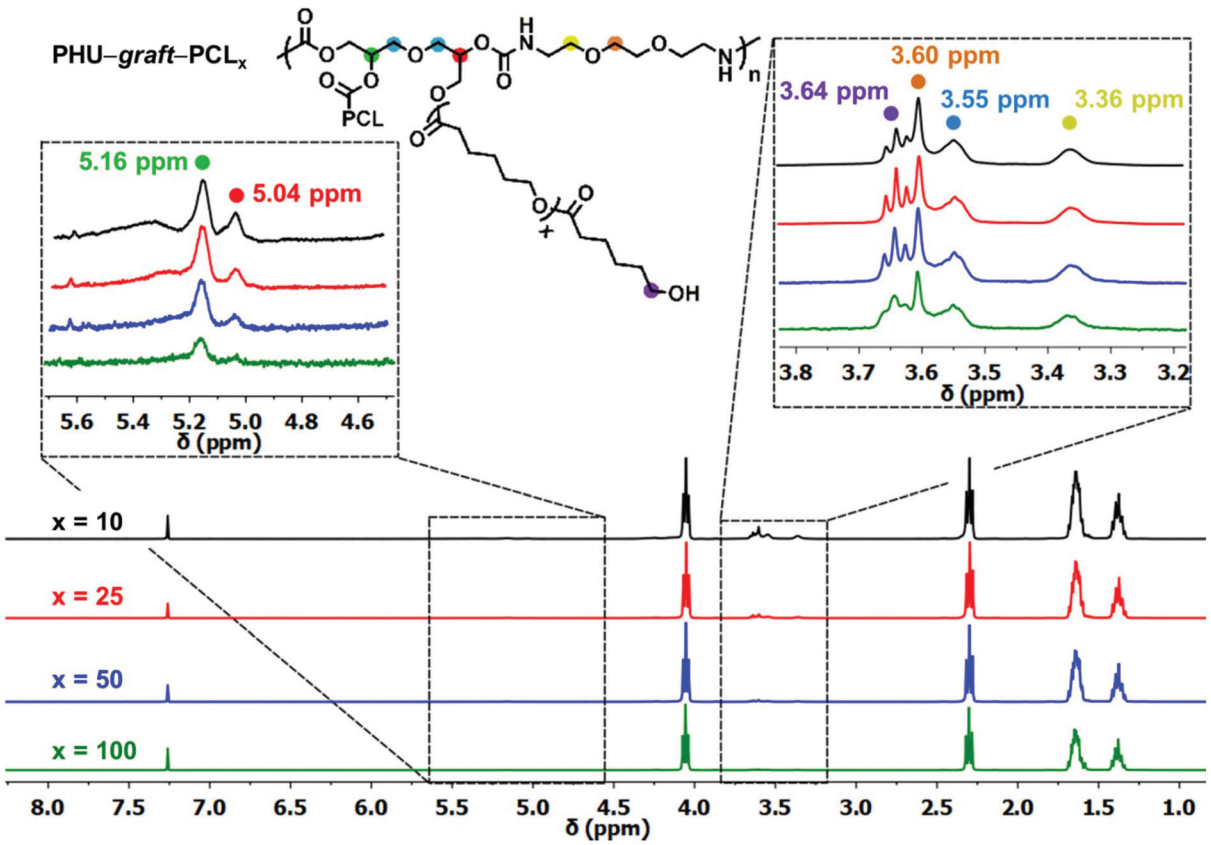

Fig. 6 Stacked ^{1}H NMR spectra (400 MHz, $CDCl_3$) of the final PHU-*graft*-PCL_x copolymers.

2-ethylhexanoic acid residue in the $Sn(Oct)_2$ catalyzed reactions, was considered highly unlikely as it should have been removed during precipitation.[55]

Overall, the kinetics of the MSA and $Sn(Oct)_2$ catalyzed reactions with varying catalyst loading, showed that the copolymers formed under $Sn(Oct)_2$ catalysis exhibited higher molar mass and lower CL homopolymer content, compared to their MSA analogues. Hence, $Sn(Oct)_2$ was selected for the rest of the study. The $CL_{100}Sn_{0.02}$ sample portrayed monomodal molar mass distribution and reached high conversion (88.5%) and M_n (64 300 g mol^{-1}) within a reasonable timeframe (8 h) while the extent of transesterification was comparably low ($Đ$ = 2.2). Therefore, the 1 : 0.02 OH : $Sn(Oct)_2$ ratio was considered the optimum. Keeping the OH : $Sn(Oct)_2$ ratio fixed at 1 : 0.02, the reactions were kinetically monitored by varying the CL : OH ratio to 10 : 1, 25 : 1, 50 : 1 and 100 : 1. The samples were again named according to the CL : OH and OH : $Sn(Oct)_2$ molar ratio. For instance, $CL_{10}Sn_{0.02}$ denotes a 10 : 1 CL : OH ratio and a 1 : 0.02 OH : $Sn(Oct)_2$ ratio. The reaction characteristics are summarized in Table 1 and the conversion, M_n and $Đ$ *vs.* time plots are presented in Fig. 5. The reactions fall into two groups depending on the CL loading of the samples. The low CL loading samples, $CL_{10}Sn_{0.02}$ and $CL_{25}Sn_{0.02}$, exhibited conversions above 90% within 2–3 h and reached their final M_n approximately at the same time. Thereafter, due to transesterification reactions, the M_n decreased continuously followed by quick increase of $Đ$ for $CL_{10}Sn_{0.02}$ and a more gradual increase for $CL_{25}Sn_{0.02}$. After 24 h the samples had gelled, similarly to what has been previously observed in graft copolymers of poly(ethylene-*co*-vinyl alcohol) and CL.[58] The samples with higher CL loadings, $CL_{50}Sn_{0.02}$ and $CL_{100}Sn_{0.02}$, reached high conversion, ≥85%, after 8 h and the M_n increased continuously during the total 24 h of reaction time. $Đ$ increased more modestly compared to the reactions with a low CL loading, with a slightly higher value for $CL_{50}Sn_{0.02}$ than $CL_{100}Sn_{0.02}$. The presence of CL homopolymer is low in all cases, Fig. S9.† Thus, it is shown that the CL loading can be varied to obtain PHU-*graft*-PCL copolymers with varying molar mass of the PCL grafts and controlled characteristics.

Synthesis of PHU-*graft*-PCL copolymers under the optimized conditions

The synthesis of the PHU-*graft*-PCL copolymers with 1 : 0.02 OH : $Sn(Oct)_2$ ratio was repeated for the four CL loadings (10, 25, 50, 100 CL monomers per –OH group) and quenched upon high conversion. The final copolymers were named PHU-*graft*-PCL_x where x signifies the theoretical number of CL repeating units per –OH group. The reaction conditions and characteristics of the final copolymers are presented in Table 2.

Side reactions were suppressed as seen from the final M_n and $Đ$ values, Table 2. The successful graft ROP of CL from the PHU was proven by ^{1}H NMR spectroscopy where the signals at 5.16 and 5.04 ppm, corresponding to the methine protons next to the esterified hydroxyls of the PHU, are detected for all the copolymers, Fig. 6. The PHU's backbone signals between 3.60–3.36 ppm and the terminal –CH_2OH of PCL at 3.64 ppm are also clearly observed. Partial overlapping of the –OCH_2CH_2O– protons of the diamine at 3.60 ppm with the terminal –CH_2OH protons of PCL at 3.64 ppm did not allow for an estimation of PCL's degree of polymerization. However, DOSY NMR experiments indubitably showed copolymer formation and the absence of copolymer/CL homopolymer blend,

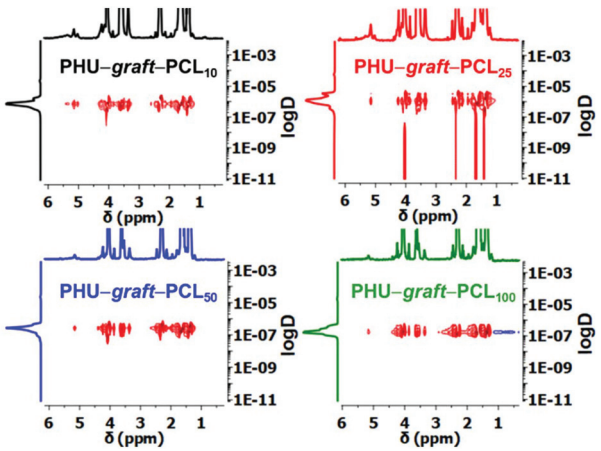

Fig. 7 DOSY NMR spectra (400 MHz, $CDCl_3$) of the PHU-*graft*-PCL copolymers.

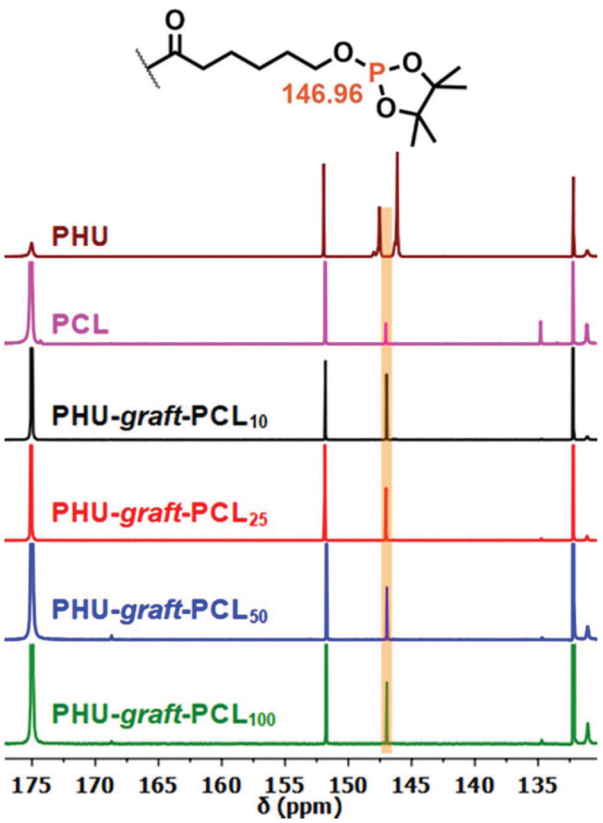

Fig. 8 ^{31}P NMR spectra of the final PHU-*graft*-PCL copolymers. All of the –OH groups of the PHU have reacted and only the terminal –OH of the PCL grafts are present.

Table 3 Thermal properties of the pure PHU and the PHU-*graft*-PCL_x copolymers[a]

x	$T_{g,\ PHU}$ [b] (°C)	$T_{g,\ PCL}$ [b] (°C)	T_m [b] (°C)	ΔH_m [b] (J g^{-1})	T_c [c] (°C)	ΔH_c [c] (J g^{-1})	X_c [e] (%)	$T_{d,5\%}$ [f] (°C)
PHU	9.6 ± 1.3	—	—	—	—	—	—	241
PCL	—	−50.2 ± 1.4	54.8 ± 0.1	68.3 ± 2.6	34.6 ± 0.3	70.8 ± 0.5	49	268
10	7.8 ± 0.3	−50.6 ± 0.7	42.6 ± 0.1	63.2 ± 0.5	16.3 ± 0.1	63.4 ± 0.9	45	288
25[d]	—	—	50 ± 0.006	71.4 ± 1.3	25.4 ± 0.2	71.5 ± 1.1	51	291
50[d]	—	—	53.4 ± 0.01	72.8 ± 1.3	29.5 ± 0.4	72.3 ± 1.4	52	291
100[d]	—	—	55.4 ± 0.2	68.7 ± 2.3	28.9 ± 0.6	67.7 ± 2.0	49	301

[a] All values are averages of triplicate measurements. [b] Determined from the second heating scan. [c] Determined from the cooling scan. [d] No T_g could be observed for either block. [e] Calculated through eqn (1). [f] Determined by TGA analysis at 5% mass loss.

as all of the ^{1}H signals are attributed to a single species with the same diffusion coefficient,[65] Fig. 7. Finally, ^{31}P NMR spectroscopy confirmed that there are no unreacted −OH groups on the PHU after polymerization, as only the terminal −OH of the PCL blocks were identified at 146.96 ppm, Fig. 8.

Thermal properties of the PHU-*graft*-PCL copolymers

The thermal properties of the PHU-*graft*-PCL copolymers were controlled by the molar mass of the PCL grafts. The melting (T_m) and crystallization (T_c) temperature and the respective enthalpies (ΔH_m and ΔH_c), increased with increased molar mass of the PCL blocks, Table 3, Fig. S10.† The PHU and PCL segments were not miscible as two discrete T_gs were observed for the PHU-*graft*-PCL_{10} copolymer, in the vicinity of the T_gs of the corresponding homopolymers. The absence of clear glass transitions in the thermographs of the other copolymers, is most likely associated to their higher degree of crystallinity (X_c) compared to PHU-*graft*-PCL_{10}. The degree of crystallinity increased with increasing molar mass of the PCL chains, yet it was slightly lower for the PHU-*graft*-PCL_{100} copolymer (49%). This is in line with previous observations of PCL displaying lower crystallinity at higher molar masses.[66,67] The onset decomposition temperature ($T_{d,\ 5\%}$) of the copolymers was in the range of 288–300 °C and, as expected, it increased with increasing molar mass of the PCL grafts, Table 3. The grafted PCL was advantageous as it offered greater thermal stability due to the more stable ester bonds compared to the thermally labile urethane linkages of the PHU.

Conclusions

Tunable polyhydroxyurethane-*graft*-poly(ε-caprolactone) copolymers with brush-like architecture were successfully synthesized through a 'grafting from' approach. Judicious selection of the PHU monomers, DGC and EDOBA, afforded a PHU that dissolved in CL at 110 °C and therefore enabled the graft ROP of CL in bulk. The system presented several features of sustainable design, solvent-free preparation of both the PHU backbone and the PHU-*graft*-PCL copolymers, combined with the biobased origin of DGC and mild reaction conditions. The polymerization reaction was robust and the molar mass of the PCL blocks was tuned by simply varying the CL : OH ratio. The thermal properties of the copolymers were controlled by the molar mass of PCL and the copolymerization was beneficial for the thermal stability, which was enhanced compared to the pure PHU. This work demonstrates that complex structures, that would otherwise be challenging to achieve, can be synthesized by utilizing polymer-in-monomer solubility. This enables the design of solvent-free systems and opens new possibilities for sustainable polymer synthesis.

Conflicts of interest

There are no conflicts to declare.

Acknowledgements

This work is financially supported by the Swedish Research Council Formas (2016-00700). Prof. Zoltán Szabò, Department of Chemistry, KTH Royal Institute of Technology, is gratefully acknowledged for all the help with the DOSY NMR experiments.

References

1 L. Maisonneuve, O. Lamarzelle, E. Rix, E. Grau and H. Cramail, *Chem. Rev.*, 2015, **115**, 12407–12439.
2 V. Schimpf, J. B. Max, B. Stolz, B. Heck and R. Mülhaupt, *Macromolecules*, 2019, **52**, 320–331.
3 F. Magliozzi, G. Chollet, E. Grau and H. Cramail, *ACS Sustainable Chem. Eng.*, 2019, **7**, 17282–17292.
4 C. Carré, Y. Ecochard, S. Caillol and L. Avérous, *ChemSusChem*, 2019, **12**, 3410–3430.
5 V. Froidevaux, C. Negrell, S. Caillol, J.-P. Pascault and B. Boutevin, *Chem. Rev.*, 2016, **116**, 14181–14224.
6 A. Boyer, E. Cloutet, T. Tassaing, B. Gadenne, C. Alfos and H. Cramail, *Green Chem.*, 2010, **12**, 2205–2213.
7 M. Bähr, A. Bitto and R. Mülhaupt, *Green Chem.*, 2012, **14**, 1447–1454.
8 M. Alves, B. Grignard, A. Boyaval, R. Méreau, J. De Winter, P. Gerbaux, C. Detrembleur, T. Tassaing and C. Jérôme, *ChemSusChem*, 2017, **10**, 1128–1138.
9 M. Tryznowski, A. Swiderska, Z. Zołek-Tryznowska, T. Gołofit and P. G. Parzuchowski, *Polymer*, 2015, **80**, 228–236.

10 J. L. J. van Velthoven, L. Gootjes, D. S. Van Es, B. A. J. Noordover and J. Meuldijk, *Eur. Polym. J.*, 2015, **70**, 125–135.
11 H. Blattmann, M. Fleischer, M. Bähr and R. Mülhaupt, *Macromol. Rapid Commun.*, 2014, **35**, 1238–1254.
12 V. Besse, F. Camara, F. Méchin, E. Fleury, S. Caillol, J. P. Pascault and B. Boutevin, *Eur. Polym. J.*, 2015, **71**, 1–11.
13 M. Blain, A. Cornille, B. Boutevin, R. Auvergne, D. Benazet, B. Andrioletti and S. Caillol, *J. Appl. Polym. Sci.*, 2017, **44958**, 1–13.
14 H. Matsukizono and T. Endo, *Macromol. Chem. Phys.*, 2017, **218**, 1–11.
15 S. Benyahya, M. Desroches, R. Auvergne, S. Carlotti, S. Caillol and B. Boutevin, *Polym. Chem.*, 2011, **2**, 2661–2667.
16 O. Lamarzelle, G. Hibert, S. Lecommandoux, E. Grau and H. Cramail, *Polym. Chem.*, 2017, **8**, 3438–3447.
17 B. Ochiai, H. Kojima and T. Endo, *J. Polym. Sci., Part A: Polym. Chem.*, 2014, **52**, 1113–1118.
18 L. Maisonneuve, A. S. More, S. Foltran, C. Alfos, F. Robert, Y. Landais, T. Tassaing, E. Grau and H. Cramail, *RSC Adv.*, 2014, **4**, 25795–25803.
19 A. Yuen, A. Bossion, E. Gomez, F. Ruipérez, M. Isik, J. Hedrick, D. Mecerreyes, Y.-Y. Yang and H. Sardon, *Polym. Chem.*, 2016, **7**, 2105–2111.
20 M. Helou, J.-F. Carpentier and S. M. Guillaume, *Green Chem.*, 2011, **13**, 266–271.
21 L. Annunziata, A. K. Diallo, S. Fouquay, G. Michaud, F. Simon, J.-M. Brusson, J.-F. Carpentier and S. M. Guillaume, *Green Chem.*, 2014, **16**, 1947–1956.
22 R. Hamiye, A. Alaaeddine, M. Awada, B. Campagne, S. Caillol, S. M. Guillaume, B. Ameduri and J. F. Carpentier, *Polym. Chem.*, 2014, **5**, 5089–5099.
23 Y.-Y. Zhang, Y. Li, X.-J. Zhou, X.-H. Zhang, B.-Y. Du and Z.-Q. Fan, *Macromol. Rapid Commun.*, 2015, **36**, 852–857.
24 B. Quienne, N. Kasmi, R. Dieden, S. Caillol and Y. Habibi, *Biomacromolecules*, 2020, **21**, 1943–1951.
25 A. Granata and D. S. Argyropoulos, *J. Agric. Food Chem.*, 1995, **43**, 1538–1544.
26 P. Furtwengler, R. Perrin, A. Redl and L. Avérous, *Eur. Polym. J.*, 2017, **97**, 319–327.
27 P. Furtwengler and L. Avérous, *Sci. Rep.*, 2018, **8**, 1–14.
28 V. Crescenzi, G. Manzini, G. Calzolari and C. Borri, *Eur. Polym. J.*, 1972, **8**, 449–463.
29 L. Maisonneuve, A.-L. Wirotius, C. Alfos, E. Grau and H. Cramail, *Polym. Chem.*, 2014, **5**, 6142–6147.
30 O. Lamarzelle, P.-L. Duran, A.-L. Wirotius, G. Chollet, E. Grau and H. Cramail, *Polym. Chem.*, 2016, **7**, 1439–1451.
31 M. Blain, L. Jean-Gérard, R. Auvergne, D. Benazet, S. Caillol and B. Andrioletti, *Green Chem.*, 2014, **16**, 4286–4291.
32 A. Cornille, M. Blain, R. Auvergne, B. Andrioletti, B. Boutevin and S. Caillol, *Polym. Chem.*, 2017, **8**, 592–604.
33 H. Tomita, F. Sanda and T. Endo, *J. Polym. Sci., Part A: Polym. Chem.*, 2001, **39**, 162–168.
34 H. Tomita, F. Sanda and T. Endo, *J. Polym. Sci., Part A: Polym. Chem.*, 2001, **39**, 851–859.
35 H. Tomita, F. Sanda and T. Endo, *J. Polym. Sci., Part A: Polym. Chem.*, 2001, **39**, 3678–3685.
36 F. Yu and R. Zhuo, *Polym. J.*, 2004, **36**, 28–33.
37 H. Alamri, J. Zhao, D. Pahovnik and N. Hadjichristidis, *Polym. Chem.*, 2014, **5**, 5471–5478.
38 A. Bossion, R. H. Aguirresarobe, L. Irusta, D. Taton, H. Cramail, E. Grau, D. Mecerreyes, C. Su, G. Liu, A. J. Müller and H. Sardon, *Macromolecules*, 2018, **51**, 5556–5566.
39 Y. Marcus, *J. Solution Chem.*, 1984, **13**, 599–624.
40 K. L. Hoy, *J. Paint Technol.*, 1970, **42**, 76–118.
41 K. L. Hoy, *The Hoy Tables of Solubility Parameters*, Union Carbide Corporation, Solvents and Coatings Materials Division, South Charleston, WV, 1985.
42 K. L. Hoy, *J. Coated Fabr.*, 1989, **19**, 53–67.
43 D. W. Van Krevelen and K. Te Nijenhuis, in *Properties of Polymers:Their Correlation with Chemical Structure; their Numerical Estimation and Prediction from Additive Group Contributions*, Elsevier B.V., New York, 4th edn, 2009, pp. 189–227.
44 E. A. Grulke, in *Polymer Handbook*, ed. J. Brandrup, E. H. Immergut and E. A. Grulke, John Wiley & Sons, Inc., 4th edn, 1999, p. 689.
45 K. B. Wiberg and R. F. Waldron, *J. Am. Chem. Soc.*, 1991, **113**, 7705–7709.
46 P. Olsén, N. Herrera and L. A. Berglund, *Biomacromolecules*, 2020, **21**, 597–603.
47 M. Labet and W. Thielemans, *Chem. Soc. Rev.*, 2009, **38**, 3484–3504.
48 W. N. Ottou, H. Sardon, D. Mecerreyes, J. Vignolle and D. Taton, *Prog. Polym. Sci.*, 2016, **56**, 64–115.
49 R. F. Storey and J. W. Sherman, *Macromolecules*, 2002, **35**, 1504–1512.
50 C. Navarro, B. Martín-Vaca, D. Bourissou, S. Gazeau-Bureau, S. Magnet and D. Delcroix, *Macromolecules*, 2008, **41**, 3782–3784.
51 R. C. Pratt, B. G. G. Lohmeijer, D. A. Long, R. M. Waymouth and J. L. Hedrick, *J. Am. Chem. Soc.*, 2006, **128**, 4556–4557.
52 N. Susperregui, D. Delcroix, B. Martin-Vaca, D. Bourissou and L. Maron, *J. Org. Chem.*, 2010, **75**, 6581–6587.
53 A. C. Albertsson and I. K. Varma, *Biomacromolecules*, 2003, **4**, 1466–1486.
54 M. Bero, B. Czapla, P. Dobrzyński, H. Janeczek and J. Kasperczyk, *Macromol. Chem. Phys.*, 1999, **200**, 911–916.
55 R. F. Storey and A. E. Taylor, *J. Macromol. Sci., Part A: Pure Appl.Chem.*, 1998, **35**, 723–750.
56 A. Kowalski, A. Duda and S. Penczek, *Macromol. Rapid Commun.*, 1998, **19**, 567–572.
57 K. Odelius and A. Albertsson, *J. Polym. Sci., Part A: Polym. Chem.*, 2008, **46**, 1249–1264.
58 H. Jiang, J. He, J. Liu and Y. Yang, *Polym. J.*, 2002, **34**, 682–686.
59 Y. Li, J. Nothnagel and T. Kissel, *Polymer*, 1997, **38**, 6197–6206.

60 A. Pascual, H. Sardon, A. Veloso, F. Ruipérez and D. Mecerreyes, *ACS Macro Lett.*, 2014, **3**, 849–853.
61 M. Baśko and P. Kubisa, *J. Polym. Sci., Part A: Polym. Chem.*, 2006, **44**, 7071–7081.
62 M. Baśko and P. Kubisa, *J. Polym. Sci., Part A: Polym. Chem.*, 2007, **45**, 3090–3097.
63 J. M. Ren, Q. Fu, A. Blencowe and G. G. Qiao, *ACS Macro Lett.*, 2012, **1**, 681–686.
64 A. Pascual, J. R. Leiza and D. Mecerreyes, *Eur. Polym. J.*, 2013, **49**, 1601–1609.
65 P. Groves, *Polym. Chem.*, 2017, **8**, 6700–6708.
66 C. G. Pitt, F. I. Chasalow, Y. M. Hibionada, D. M. Klimas and A. Schindler, *J. Appl. Polym. Sci.*, 1981, **26**, 3779–3787.
67 P. Skoglund and Å. Fransson, *J. Appl. Polym. Sci.*, 1996, **61**, 2455–2465.